Immunoscintigraphy of Ovarian Cancer with Indium-111-Labeled OV-TL 3 F(ab')$_2$ Monoclonal Antibody

Leon F.A.G. Massuger, Peter Kenemans, Roland A.M.J. Claessens, René H.M. Verheijen, Charles P.T. Schijf, Simon P. Strijk, Lambert G. Poels, René G.C.M. van Hoesel, and Frans H.M. Corstens

Departments of Obstetrics and Gynecology, Nuclear Medicine, Radiology, Cell Biology and Histology, and Medical Oncology, University Hospital Nijmegen, Nijmegen, The Netherlands and Department of Obstetrics and Gynecology, Free University Hospital, Amsterdam, The Netherlands

The safety and diagnostic accuracy of immunoscintigraphy with the indium-111-labeled monoclonal antibody OV-TL 3 F(ab')$_2$ (^{111}In-OV-TL 3 F(ab')$_2$) for diagnosis and follow-up of ovarian cancer was prospectively studied in 31 patients. Planar and SPECT scintigraphy were performed up to 4 days after i.v. injection of 140 MBq ^{111}In-OV-TL 3 F(ab')$_2$. Surgical evaluation was possible in 22 out of 31 patients. Imaging results were compared with X-ray computed tomography, ultrasound, and CA 125 serum level using the histologically confirmed surgical findings as a "gold standard." Apart from a transient rash observed in two patients, no other immediate or delayed adverse reactions were observed. Within the surgically evaluated group, ovarian cancer lesions were detected in 16 out of 17 patients (94%). Of 45 distinct tumor deposits found at operation, 67% were detected and localized with immunoscintigraphy while X-ray computed tomography and ultrasound visualized 53% and 23%, respectively.

J Nucl Med 1990; 31:1802–1810

Ovarian cancer is still one of the leading causes of cancer death in women in the western world (*1*). The overall five-year survival rate is ~30% (*2*). The silent spread of ovarian cancer within the abdominal cavity and the lack of a suitable technique to detect this spread are the main reasons that 70% of the patients are found to have advanced disease (FIGO Stage III or IV) at the time of diagnosis (*3*).

Current therapy mostly combines surgical debulking with combination chemotherapy (including cisplatin), leading to a considerable percentage (68%) of clinical responses (*4*). A major problem is the inability to unequivocally determine complete remission with non-invasive methods. Recently developed serum tumor markers, e.g., CA 125 (*5*), can be used as warning signals, roughly reflecting the course of disease with a high rate of false-negatives at the time of second-look operation (*6*). New techniques must be developed that allow determination of the actual disease status both in primary patients as well as in those suspected to have persistent or recurrent disease.

Conventional noninvasive tools to assess the presence and spread of abdominal and pelvic malignancies include ultrasound (US), X-ray computed tomography (CT) and magnetic resonance imaging (MRI). Until now, these diagnostic modalities do not provide sufficient information about the actual disease status of an individual patient. CT is unable to detect small-sized tumors in many abdominal and pelvic localizations. The overall sensitivity for different tumor sites is 40% (*7,8*). The sensitivity of US and MRI for the detection of distinct ovarian carcinoma tumor deposits has not yet sufficiently been established.

Immunoscintigraphy (IS) using monoclonal antibodies (MAbs) has been proposed as a useful means of detecting residual or recurrent ovarian cancer (*9,10*). Various antibodies and radionuclides have been used (*9–16*). The majority of the tumor imaging studies with labeled MAbs have been performed with radionuclides of iodine (*17*). Those radioiodinated antibodies are subject to in vivo dehalogenation (*18*). Radioiodination techniques are now frequently being replaced by chelate binding metallic radionuclides, such as indium-111 (^{111}In) or technetium-99m.

The MAb used in this study, OV-TL 3, developed at the University of Nijmegen (*19*), has shown encouraging preliminary results in ovarian cancer patients (*20*).

In the present study, F(ab')$_2$ fragments of the MAb were chosen. The goals of the present prospective study were (a) to determine the safety of intravenously administered ^{111}In-labeled OV-TL 3 F(ab')$_2$ and (b) to evaluate its diagnostic accuracy in imaging patients with ovarian cancer.

Received Nov. 21, 1989; revision accepted May 14, 1990.

For reprints contact: Prof. Dr. F.H.M. Corstens, Dept. of Nuclear Medicine, University Hospital Nijmegen, 6500 HB Nijmegen, The Netherlands.

MATERIALS AND METHODS

Monoclonal Antibody

OV-TL 3 is a murine MAb of the IgG_1 subclass that recognizes a cell surface antigenic determinant (OA 3) present on most ovarian carcinomas. OA 3 is a glycoprotein with apparent weights of 20 and 40 kilodaltons. The antibody was generated by immunization of BALB/c mice with a cell suspension prepared from an endometrioid ovarian carcinoma (*19*). Using the immunofluorescence technique, OV-TL 3 was stained on frozen sections from more than 90% of human ovarian carcinomas of various histologic types (*19,21*). Occasional reactivity has been seen with several other gynecologic and non-gynecologic tumors (*19,22*). Within a limited number of normal tissues tested, no cross reactivity has been seen apart from reactivity with epithelium of the female genital tract (*19*). In contrast to many other ovarian cancer-associated antigens, e.g., CA 125 (*5*) and HMFG2 (*23*), the antigen recognized by OV-TL 3 could not be detected in serum. The MAb fragment used was provided by Centocor Inc., Malvern, PA and approved for human use as an investigative new drug by the Federal Drug Administration, USA. Approval was also obtained from the National Board of Health in the Netherlands and the Human Research Review Committee of the University Hospital Nijmegen.

The $F(ab')_2$ fragments were prepared by direct pepsin digestion of the OV-TL 3 IgG. The crude $F(ab')_2$ was subsequently purified by cation-exchange chromatography on S-Sepharose fast flow.

Radiolabeling

The antibody fragment was radiolabeled with ^{111}In, using diethylenetriaminepentaacetic acid (DTPA) bicyclic anhydride as a chelating agent (*24*).

OV-TL 3 $F(ab')_2$-DTPA was supplied in a two-vial kit as a sterile non-pyrogenic solution. The first vial contained 1.0 mg of OV-TL 3 $F(ab')_2$-DTPA in 1 ml of 10 m*M* sodium phosphate, 0.15 *M* sodium chloride, 10% w/v maltose, pH 6.5, with no preservatives. The contents of the first vial was added to the second vial containing 1.0 ml of 0.2 *M* sodium citrate (pH 5.0) in order to acidify the antibody-DTPA complex prior to the labeling with ^{111}In. The antibody was radiolabeled by adding 185 MBq of sterile pyrogen-free ^{111}In-chloride (Amersham Intl., Amersham, UK). The final preparation contained 1–2 DTPA molecules per antibody molecule. Prior to injection the preparation was sterilized by filtration.

Quality Control

Instant thin-layer chromatography (ITLC) was used to determine the labeling efficiency of the radiolabeled antibody. For this purpose, Gelman ITLC-SG strips were used with 0.1 *M* sodium citrate (pH 5.0) solution as solvent.

Immunoreactivity of the $F(ab')_2$-DTPA immunoconjugate was tested with NIH:OVCAR-3 cells in an ELISA and compared to the reactivity of unconjugated intact OV-TL 3.

Routine binding of the radiolabeled fragment to ovarian carcinoma cells was tested with a competitive binding assay, using glutaraldehyde (0.25%) fixed NIH:OVCAR-3 ovarian carcinoma cells (*25*) as a solid phase. A fixed concentration of labeled antibody (50 ng/ml) was incubated (4 hr, room temp.) in the presence of various concentrations of cold intact OV-TL 3. Binding of ^{111}In-labeled OV-TL 3 $F(ab')_2$ was compared to that of radioiodinated whole IgG OV-TL 3. From these studies, the affinity constant of the injected preparation was determined (*26*).

Patients

All patients enrolled in the study (n = 31) were either highly suspected of having ovarian cancer (n = 15) or had cytologic or histologic evidence of ovarian cancer (n = 16).

Prior therapy did not restrict admission to the study as long as the last course was administered at least 3 wk prior to study entry and hematologic recovery had occurred. Patients with known allergy to murine antigens, life-threatening infection, allergic diathesis or diagnosis of a second malignancy, other than treated squamous/basal cell carcinoma of the skin, were excluded. Patients with prior administration of murine MAb were also excluded from the study. The procedure was explained to each patient and informed consent was obtained prior to study entry. Some characteristics of the patients are listed in Table 1. The mean age was 62.3 yr (median age 64 yr, range 44–78 yr). No patient was studied twice. Fourteen patients had received chemotherapy for epithelial ovarian cancer prior to immunoscintigraphy. Surgery was performed on 22 of the 31 patients.

Patient Studies

Medical history was taken and physical examination was performed in each patient prior to i.v. injection of the antibody. Blood was drawn for a complete blood count, WBC, differential WBC, platelet count and serum biochemical profile. These measurements were repeated at 24 and 48 hr after injection and again after three weeks. An electrocardiogram, chest radiograph, and a CA 125 serum level (Table 1) were also obtained as part of the pre-antibody injection evaluation.

In all patients studied, standardized X-ray CT with the aid of oral and i.v. contrast agents was performed within a period of seven days from administration of the radioimmunoconjugate. Abdominal and pelvic scans of 8 mm thickness at 8 mm intervals were obtained from the level of the diaphragm to the perineum with a third-generation CT-scanner (Siemens Somatom 3, Hoffman Estates, IL). All CT scans were evaluated by one radiologist, unaware of immunoscintigraphic or surgical results. In 20 out of 22 operated patients, US was performed as a routine preoperative screening using a Diasonics DRF 100 sector scanner (Les Ulis, France).

All patients received ~148 MBq (122–162 MBq) of ^{111}In-labeled MAb (1.0 mg). A skin test was not performed. The antibody preparation was diluted in 5 ml of saline and infused over a 5-min period of time into the cephalic vein. Vital signs (blood pressure, pulse rate, temperature and breathing frequency) were measured frequently up to 3 hr after injection and again at 24 and 48 hr.

Both planar scintigraphy and SPECT were performed using the same rotating single-head gamma camera with a parallel-hole medium-energy collimator (Siemens, type Orbiter, Hoffman Estates, IL). Planar scintillation camera images were recorded at 4, 24, 48, 72, and 96 hr postinfusion. Digital acquisition was recorded on a Siemens Scintiview data processing system. Both 173-keV and 247-keV gamma-ray peaks of ^{111}In with symmetric 20% windows were used to record anterior and posterior views of the chest, abdomen, and pelvis with a preset time of 5 min. An additional image of the pelvis, with the patient sitting above the camera surface leaning

TABLE 1
Characteristics of 31 Prospectively Investigated Patients Suspected for or Known to Have Ovarian Cancer

Patient no.	Age (yr)	FIGO stage	Primary carcinoma	Serum CA 125 (U/ml)	Surgery performed
1	75	III	serous	120	+
2	53	IV	serous	7200	+
3	44	III	serous	290	–
4	54	III	serous	40	+
5	67	III	endometrioid	320	–
6	61	III	serous	5200	+
7	71	IIC	endometrioid	10	+
8	56	III	serous	430	+
9	56	I	serous	130	+
10	70	IV	adenocarc.	450	+
11	77	III	adenocarc.	4400	–
12	53	IIIC	serous	14000	+
13	56	IC	serous	7700	–
14	69	IV	serous	2900	+
15	50	III	serous	880	+
16	59	III	serous	2000	–
17	67	III	adenocarc.	890	+
18	78	III	endometrioid	120000	–
19	62	III	serous	350	+
20	64	III	serous	57	–
21	73	IV	serous	1800	–
22	69	III	serous	460	–
23	71	IA	serous borderl.	7.5	+
24	56	IV	adenocarc.	1800	+
25	64	—	benign	15	+
26	61	IV	adenocarc.	1200	+
27	60	IIIC	endometrioid	160	+
28	57	IIIC	serous	2800	+
29	77	—	coloncarc.	11	+
30	66	—	benign	8.2	+
31	57	—	benign	14	+

Cut-off value for CA 125: 35 U/ml.

backwards, was also recorded. Typical planar images had 1,000,000–2,900,000 counts at 4 hr and 500,000–900,000 counts at 96 hr. Scans were interpreted by two nuclear medicine physicians unaware of the results of the patients' prior evaluations. Images were interpreted as positive when evaluation of all the images recorded over time consistently showed areas of localized increased uptake, not corresponding to sites with known physiologic uptake (bone, liver, spleen, kidney, bladder and bowel). Bowel uptake was discriminated from tumor uptake by evaluation of the pattern of increased localized activity over time.

SPECT studies were performed at 24, 48, and 72 hr post-injection (p.i.). The same peak-energy and window settings were used as for planar imaging. Sixty-four frames were recorded through 360° with recording time of 45 sec per frame. Typical frames at 24 hr had 200,000–320,000 counts and 100,000–170,000 counts at 72 hr. Digital acquisition was recorded on a Microdelta Computer system (Siemens, Hoffman Estates, IL). For each recording, 6.3-mm thick transverse, coronal, and sagittal sections were reconstructed using a Ramp filter and a cut-off frequency of 0.4 Nyquist. SPECT images were interpreted as positive when areas of increased uptake were seen in at least two out of three studies, not corresponding to sites with known physiologic uptake.

Surgery was performed on 22 out of 31 patients between 5 and 7 days after MAb injection. At surgery, the whole abdomino-pelvic cavity was carefully checked for abnormalities. All suspect tissues were either completely removed or biopsies were taken. All tissues obtained at surgery underwent histopathologic examination. Furthermore, scintiscans were made of all resected tissues, using the same gamma camera as was used for the patient studies.

Imaging results were evaluated in two different ways using the histologically confirmed surgical findings as a "gold standard." The detection of ovarian cancer positive and negative patients was assessed in the 22 operated patients and compared with CT, US, and CA 125 serum level. However, the actual diagnostic accuracy of IS with ^{111}In-OV-TL 3 F(ab')$_2$ was assessed by evaluating the detection and localization rate of distinct tumor deposits found at operation. Tumor deposits smaller than 1 cm in diameter, including peritoneal carcinosis, were left out of this second analysis.

RESULTS

Labeling Efficiency and Immunoreactivity

Within 1 hr prior to MAb injection, labeling efficiency was determined by ITLC. The result was always better than 98%. Immunoreactivity testing using an ELISA indicated that 50% of the maximum binding of the OV-TL 3 F(ab')$_2$-DTPA was obtained at a concentration not significantly higher than that with intact OV-TL 3. Displacement studies were performed as described. The affinity constant of the injected preparation ranged from 1 to 4 × 10^8 1/mol, being in the same range as for the ^{125}I-labeled OV-TL 3 (whole IgG).

Adverse Reactions

During antibody infusion, none of the patients showed any side effects. Vital signs remained stable up to 48 hr after injection in all patients. In 2 of the 31 patients studied, a transient skin rash was observed 30 hr after injection of the antibody. The rash was limited to the legs and the lower abdomen and disappeared after 48 hr. The occurrence of this rash could not be explained in any other way than by the administration of the radiopharmaceutical. No other immediate- or delayed-type adverse reactions were observed. Within the first 3 wk after injection of the antibody, no major alterations were observed in biochemical and hematologic serum profiles.

Imaging Results

Visualization of the blood pool was greatest in the first few hours after MAb injection. In some patients, it was still visible at 24 hr but never on the 48-hr images (Fig. 1). Liver and spleen uptake remained high in all subsequent scintiscans. Some kidney uptake was usually seen at 4 hr, increased up to 24 hr, but was markedly diminished at 96 hr after injection. Bone (marrow) uptake resulted in visualization of pelvis, vertebrae,

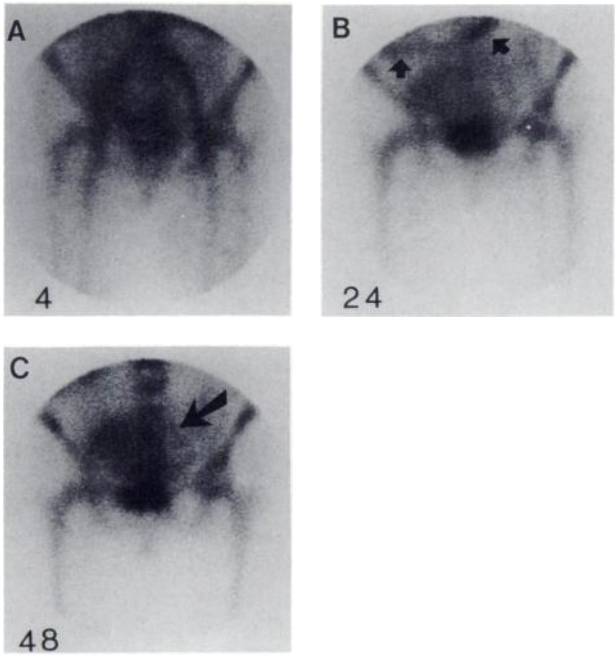

FIGURE 1
Anterior planar pelvic images 4, 24, and 48 hr p.i. of a 72-yr-old patient suspected for ovarian cancer with a palpable tumor in the right pelvis. Up to 24 hr p.i., the blood pool is clearly visible. Arrows on the 24-hr image indicate bowel uptake. From 24 hr onwards, localized uptake in the right pelvis is seen (arrow 48-hr image). At operation a large ovarian carcinoma was found in the right pelvis.

femurs, ribs, and other bones when scans were performed outside the trunk. The bone structures were helpful as orientation marks in identifying sites with increased uptake (Fig. 1). Visually, bone (marrow) uptake remained at a constant level in all images.

From 24 hr after injection, accumulation of the radionuclide in the large bowel was often seen (Fig. 1). One patient with bowel obstruction showed a string of increased uptake in the bile duct region 1 hr after decompression of the abdomen by paracentesis of 6-liter ascites (Fig. 2).

Patients with ascites showed scintigraphs with relative photopenic areas gradually filling in throughout the study (Fig. 2). This increasing activity could only be identified by planar imaging. SPECT did not show any sign of ascites.

In all patients, CT scan results were compared with immunoscintigraphic results. In addition, comparison between IS, CT scanning, US, and operative findings was possible in 22 patients (see Table 3). Of all 31 patients prospectively studied, 26 had positive images at scintigraphy. Sixteen of these 26 were proven to be correctly positive at operation. Another 9 of these 26 IS-positive patients had clinical or radiologic signs of tumor presence. The only patient with a false-positive scintigraph was found to have a colon carcinoma at operation. This tumor was immunohistochemically negative for OV-TL 3. The increased level of activity uptake in this colon tumor was confirmed when images were made of the resected specimen. Five patients had a negative scintigraph. All of these patients were operated and four of these proved to be true negatives (three benign tumors, one negative second-look laparotomy). Only one patient had a false-negative scintigraph. In this patient, a large ovarian cyst with a microscopic focus of borderline malignancy was detected at operation.

In the 22 surgically treated patients, there was good agreement between IS and histologic findings as to the presence of ovarian cancer (Table 2). In the group of patients with positive histology, only one patient was negative at scintigraphy, whereas in the group with negative histology only one patient (the patient with colon carcinoma) was positive at scintigraphy. Highest sensitivity for the detection of ovarian cancer positive patients was obtained with IS (94%). The sensitivity for the detection of ovarian cancer with CT, US, and CA 125 serum level was 82%, 73%, and 88%, respectively. There was a clear difference in specificity, 20% for CT and US and 80% for IS as well as for the CA 125 serum level.

For the 22 surgically treated patients, a total number of 45 distinct tumor localizations could be evaluated,

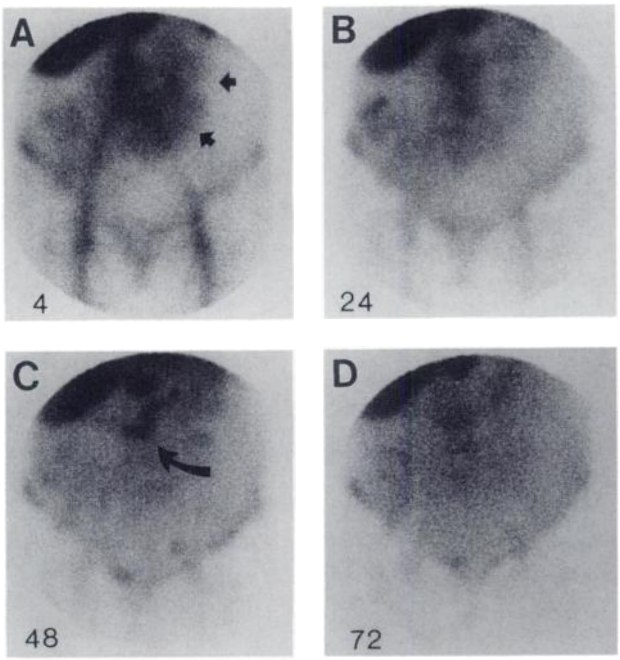

FIGURE 2
Accumulation of activity over time in ascites in a patient with ovarian cancer. Localized uptake, indicating metastatic ovarian cancer, was seen from 4 hr onwards (small arrows). The photopenic area next to the tumor deposit shows a relative increase of activity over time. One hour after paracentesis of ascites (48 hr p.i.), causing a marked decompression of the abdomen, a string of localized uptake (probably of biliary origin) could be seen in the upper abdomen (arrow 48-hr image).

TABLE 2
Detection of Ovarian Cancer Positive and Negative Patients with ^{111}In-OV-TL 3 F(ab')$_2$ in 22 Operated Patients

	IS		CT		US		CA 125	
	Pos.	Neg.	Pos.	Neg.	Pos.	Neg.	Pos.	Neg.
Positive Hist.	16	1	14	3	11	4	15	2
Negative	1	4	4	1	4	1	1	4
Sensitivity	94%		82%		73%		88%	
Specificity	80%		20%		20%		80%	

Cut-off value for CA 125: 35 U/ml.
IS = immunoscintigraphy; CT = computed tomography; US = ultrasound; and Hist. = histopathological examination.

which proved to be positive for ovarian carcinoma at histology (Table 3). Peritoneal carcinosis (seven patients) was left out of this analysis. Furthermore, liver and lymph node metastases were evaluated separately because of the lack of a histologic gold standard. Of 45 tumor-positive sites, only 23% could be detected by US. CT was able to detect 53%, whereas IS detected and localized 67% of the tumor-positive sites.

TABLE 3
Localization and Detection of Tumor-Positive Sites in 22 Surgically Evaluated Patients Suspected of Ovarian Carcinoma (Excluding Liver and Lymph Node Metastasis and Peritoneal Carcinosis)

Patient no.	No. of tumor sites	IS		CT		US	
		TP	FP	TP	FP	TP	FP
1	1	1	0	1	0	1	0
2	4	3	0	2	0	1	0
4	0	0	0	0	0	0	0
6	2	2	0	2	0	ND	
7	1	1	0	1	0	0	0
8	3	2	0	3	0	ND	
9	4	3	0	2	1	1	0
10	2	1	0	1	0	0	0
12	4	2	0	2	0	1	0
14	3	2	0	2	0	1	0
15	3	2	2	2	0	1	0
17	3	1	0	0	0	0	0
19	4	3	0	2	0	1	0
23	1*	0	0	0	0	0	0
24	4	2	0	2	0	1	0
25	0	0	0	0	2	0	1
26	3	2	1	0	1	0	0
27	1	1	1	0	0	0	0
28	2	2	0	2	0	1	0
29	0†	0	1	0	2	0	1
30	0	0	0	0	1	0	1
31	0	0	0	0	1	0	1
Total	45	30/45 (67%)	5	24/45 (53%)	8	9/40 (23%)	4

* Borderline malignancy.
† Colon carcinoma.
IS = immunoscintigraphy; CT = computed tomography; US = ultrasound; TP = true-positive; FP = false-positive; and ND = not done.

Two patients demonstrated accumulation of tracer in the uterus, already clearly visible at 4 hr p.i. This increased uptake was confirmed when images were made of the resected specimen.

Because of the very high radioactivity of normal liver tissue, small liver metastases were never visualized. However, larger metastases were visualized as cold defects in the normal liver. When CT was used as a reference, only two out of nine cases of liver metastases were visualized as cold defects with IS.

Most of the patients with advanced ovarian cancer had tumor spread to the omentum. These omental metastases could clearly be localized by SPECT imaging (Fig. 3), whereas neither CT nor US could conclusively identify these tumor deposits. With respect to these omental tumor deposits, SPECT clearly proved to be superior over planar imaging.

In eight patients, lymph nodes were found to be enlarged at surgery. Most of these nodes were not removed; thus, in most of these possible lesions a histologic gold standard was lacking. Only two out of these eight possible lesions were detected with IS (see Fig. 4), whereas CT scans detected four enlarged nodes.

Using a cut-off level of 35 U/ml, 25 out of 31 patients showed positive CA 125 serum levels prior to injection (Table 1). Overall there was a good correlation between histology, IS results, and CA 125 serum level (Table 2). However, one patient with a positive CA 125 level had true-negative IS results and one patient with a negative CA 125 serum level had true-positive IS results.

DISCUSSION

In this study, the safety and diagnostic accuracy of IS using a new ^{111}In-labeled MAb fragment OV-TL 3 F(ab')$_2$ in ovarian cancer patients were evaluated. Except for a transient rash in two patients no other immediate or delayed adverse reactions were observed. Overall, IS detected and localized 30 out of 45 distinct tumor deposits in 22 surgically treated patients, which was more than the number of sites detected with CT or US (Table 3).

Compared with other MAbs used for IS in ovarian cancer patients, OV-TL 3 was reported to be highly selective for ovarian carcinoma cells with a sensitivity of more than 90% (*19,21,22,27*). In contrast to other antibodies, e.g., OC 125, the antigenic determinant associated with OV-TL 3 is not detected in patients' serum. Thus, the theoretical problem of preliminary antibody loss by complex formation in the blood pool cannot take place. However, in several studies using a shed antigen interference of circulating antigens or an-

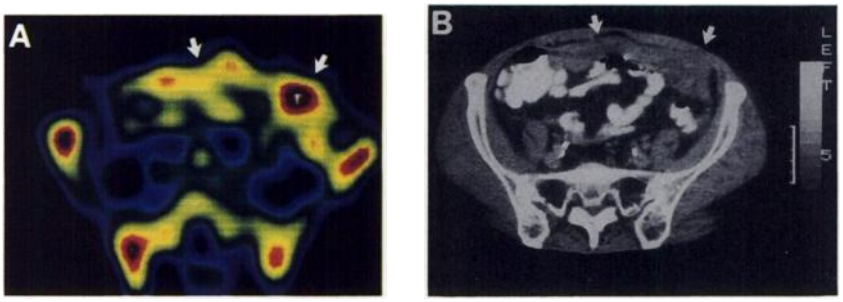

FIGURE 3
Transverse SPECT image 48 hr p.i. and corresponding CT scan of the lower abdomen in a patient with omental metastases of ovarian cancer. Increased activity is seen in the pelvic bones and the tumorous omentum (arrows).

tibody-antigen complexes on the actual tumor detection has not been persuasively demonstrated (*28,29*).

In this study, $F(ab')_2$ fragments of the MAb were chosen because, with respect to radioimaging, they seemed to be a good compromise between the rapidly cleared Fab' fragments and the slowly cleared whole IgG (*30*).

The $F(ab')_2$ fragments used were radiolabeled with ^{111}In. Tumor imaging with MAbs is improved by using ^{111}In because of its suitable physical characteristics (half-life and gamma energy) and its faster blood clearance compared with ^{131}I-labeled antibodies, resulting in higher tumor-to-background image contrast (*31,32*).

Visual interpretation of the images was not hampered by high activity in the vessels at 24 hr and later. Activity measured in blood samples 24 and 48 hr postinjection had decreased to ~5% and 2% of the injected dose per liter, respectively. With ^{111}In used as a label, high activity in liver, spleen, and kidneys was seen. Visually, the high liver and spleen uptake remained stable during the whole 5-day period of the study, whereas a visual decrease in kidney uptake was observed. High liver and spleen uptake compromises imaging of deposits within or near these organs. Consequently, diaphragmatic tumor deposits were never detected with the radioimmunoconjugate used in this study. In only two out of nine patients, liver metastases were visualized with IS. These metastases were seen as cold spots within the radioactive liver tissue. However, according to our definition of positive scintigraphic results, picking up cold lesions should not be interpreted as MAb detection of tumor deposits. One should not be surprised by this result since the uptake of the radionuclide in tumorous tissue on average is far below that in normal liver tissue. The presence of cold defects may still provide some information as to the state of the disease in the liver.

Activity in ascites obscured localized intraabdominal tumor sites. On the 4-hr images, ascites was seen as photopenic areas (Fig. 2). The uptake in these areas was markedly progressive from 24 hr onwards, compromising planar tumor detection in those areas. The problems associated with ascitic uptake were not encountered when SPECT images were interpreted.

Artifacts were produced by activity uptake in the large bowel (feces) and bladder (urine). The major route of elimination of activity was the urinary tract (~16% injected dose in 96 hr). In many patients, bowel uptake was seen 24 hr after injection (~3% injected dose in feces in 96 hr). The use of laxatives during the study and voiding prior to each pelvic imaging were necessary to reduce misleading false-positive results.

In one patient presenting with bowel obstruction, a string of activity could clearly be seen in the bile duct region after decompression by paracentesis of ascites (Fig. 2). This observation indicates that part of the bowel uptake may be the result of hepatobiliary transport of ^{111}In into the intestines. The nonspecific bowel uptake may account for some of the false-positive results that occurred with this radioimmunoconjugate (Table 3).

When interpreting images with IS, one wants to discriminate between tumor activity and aspecific localization of activity. To identify aspecific localization in vessels and bowel, one has to compare images recorded over time. Vascular activity can easily be discriminated when 4-hr images are compared with later images, while comparison of 24-hr and later images helps to identify bowel uptake.

An important goal of this prospective study was to test the value of IS in whether it can benefit a given patient by providing information additional to CT and US. With respect to the presence of ovarian cancer, the

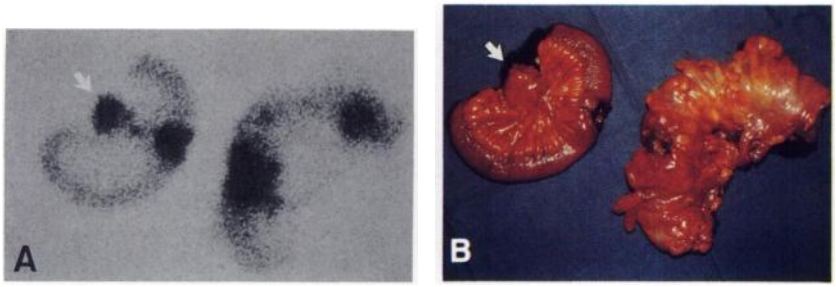

FIGURE 4
Gamma camera image and photograph of the resected specimen of a patient with recurrent ovarian cancer, 7 days postinjection. Localized uptake was seen in the tumorous parts of small and large bowel. Note the increased activity in an enlarged regional lymph node (arrows).

sensitivity of detection in this study was 94% (Table 2). This is in the same range as obtained with several other ovarian cancer-associated MAbs (*11,34,35*). The sensitivity for malignancy using CT, US, and CA 125 serum level were all just slightly lower. However, the specificities of these four diagnostic tools in detecting patients with ovarian cancer were clearly different. IS and CA 125 level had a specificity of 80%, whereas CT and US only obtained 20% specificity. In comparison with the use of the CA 125 serum assay, an important advantage of scintigraphy with OV-TL 3 $F(ab')_2$ is its ability to show the localization and extent of deposits of ovarian carcinoma.

Evaluation of the detection and localization of distinct tumor-positive sites provides a better insight in the potentials of this diagnostic tool for the detection of residual or recurrent tumor. Peritoneal carcinosis, liver, and lymph node metastasis were left out of this evaluation. With ^{111}In-labeled OV-TL 3 $F(ab')_2$, 67% of the tumor-positive sites could be detected and localized. This was in the same range as the detection and localization rate obtained in both the retrospective and prospective study of Chatal in ovarian cancer patients using ^{131}I-labeled OC 125 (*35*). With CT and US, only 53% and 23% of the tumor sites could be detected and localized. Compared to CT, US did not provide additional information in any of the patients. The localization and detection rate of tumor sites with CT was in line with literature data (*7,8*). Ultrasound was performed as a routine non-standardized preoperative screening. This may explain its very low detection rate obtained in this study. The detection and localization rate of 67% using IS, refers to the detection of primary tumors, local recurrences and intraabdominal tumor lesions larger than 1 cm in diameter. For liver (n = 9) and lymph node metastases (n = 8), no pathologic proof was available. If these possible deposits were also taken into account, detection and localization rate would decrease to 55% (34/62). Peritoneal carcinosis was never detected by SPECT, whereas with planar scintigraphy peritoneal carcinosis was only indicated by the presence of ascites, which was the case in seven patients. In contrast to MAb-guided IS, both US and CT lack (malignant) tissue specificity and cannot distinguish between malignant and benign tumor nor between recurrent tumor and postoperative changes. This may explain the relatively high number of false-positive results with CT and US (Table 3).

In one patient with a large colon carcinoma, localized uptake was seen in the tumor. In contrast to accumulation of tracer in ovarian cancer patients, localized uptake was already seen 4 hr p.i, suggesting local hyperaemia. At immunohistochemical evaluation, this tumor was found to be negative for the OV-TL 3 defined antigenic determinant. Possible explanations for this apparently aspecific uptake of ^{111}In in a nonovarian tumor are:

1. The level of antigenic determinants for OV-TL 3 in this tumor is too low to be detected immunohistochemically.
2. Enhanced vascular permeability, leading to accumulation of these radiolabeled macromolecules, as observed in inflammatory processes after injection with ^{111}In-labeled polyclonal IgG (*36*).
3. A tissue environment within this tumor, with an elevated phagocytic activity, resembling the RES system, of which high nonspecific uptake of ^{111}In is already known.

These mechanisms may also provide additional explanation for the aspecific accumulation of ^{111}In in the uterus (two patients), which was also seen by Hunter et al. using ^{111}In-labeled OC 125 (*16*).

Within the analysis of ovarian cancer positive or negative patients, there was only one false-negative result. In this patient, a large ovarian cyst with a microscopic focus of borderline malignancy was found at operation. If this patient was left out of the evaluation, sensitivity for the detection of ovarian cancer positive patients within this study would raise from 94% to 100%.

The smallest tumor deposit detected with IS was a metastasis in the bladder wall with a diameter of 1.5 cm. This metastasis could not be conclusively detected with CT, nor did the CA 125 serum level indicate tumor. To detect this metastasis with IS, the bladder had to be rinsed and refilled with saline (Fig. 5). With hemicystectomy all malignant tissue could be removed, thus indicating the clinical importance of IS in this patient.

In planar imaging of pelvic localizations of ovarian carcinoma, posterior pelvic and sitting images were the most informative. However, in pelvic and abdominal IS with ^{111}In-labeled OV-TL 3 $F(ab')_2$ SPECT is an

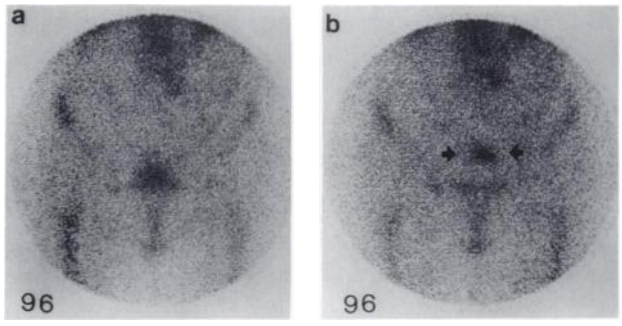

FIGURE 5
Localized uptake in a metastasis of an ovarian carcinoma in the bladder wall. Anterior pelvic images at 96 hr p.i. In the left image (a), it is impossible to discriminate urinary activity from tumor uptake. After recording this image, the urinary bladder was rinsed and refilled with saline. A subsequent image (b) showed localized uptake in the upper bladder wall. The presence of a metastasis of an ovarian carcinoma in the roof of the bladder was confirmed by pathologic examination.

essential procedure. Omental and subcutaneous metastasis as well as tumor deposits in the lower pelvic region could only be correctly localized with SPECT.

In this study, all patients were injected with 1 mg of OV-TL 3 $F(ab')_2$. Recent publications indicate that even better results may be obtained with higher doses of antibody (*37*).

Intraperitoneal injection of the antibody may enhance tumor uptake in intraabdominal tumor lesions (*38*). The i.p. route would additionally provide the opportunity of clearing the abdominal cavity of disturbing ascites. Furthermore, it may also decrease the disturbing uptake in liver and spleen, allowing visualization of tumor in the upper abdominal region. However, multiple i.p. adhesions and retroperitoneal tumor deposits, both often seen in patients with recurrent ovarian carcinoma, make the i.p. route less favorable.

Immunoscintigraphy using ^{111}In-labeled OV-TL 3 $F(ab')_2$ proved a useful tool in the detection of primary and locally recurrent ovarian cancer. Optimal interpretation of IS was achieved when subsequent images, recorded over time, were compared with each other. Overall best images were obtained 48 hr p.i. Immunoscintigraphy provided additional information in patients with false-positive as well as false-negative CA 125 serum levels. Furthermore, IS detected more tumor deposits than CT scanning in 6 out of 22 operated patients. Besides the gain in the number of detected tumor deposits, IS, using tumor-associated MAbs as a vehicle, provides more specific information with regard to the nature of the detected lesions. This important advantage may simplify the therapeutic management of ovarian cancer patients.

ACKNOWLEDGMENTS

The authors thank Centocor Inc., Malvern, PA for the supply of the antibody fragment. We are grateful to Drs. O. Boerman and W. v.d. Broek for their expert technical assistance in the labeling and quality control of the antibody fragments. We thank A. Meeuwis and D. Immerzeel for imaging, J. Wijnen for the expert photographic illustration, and A. Bakker for preparation of the manuscript.

REFERENCES

1. Green MH, Clark JW, Blayney DW. The epidemiology of ovarian cancer. *Semin Oncol* 1984; 11:209–226.
2. Cutler SJ, Myers MH, Green SG. Trends in survival rate of patients with cancer. *N Engl J Med* 1975; 193:122–124.
3. Barber HK. *Ovarian carcinoma.* New York Masson Inc.; 1982.
4. Neit JP. Combination chemotherapy in the treatment of advanced ovarian carcinoma. PhD Thesis, Utrecht, 1983.
5. Bast RC, Feeney M, Lazarus H, et al. Reactivity of a monoclonal antibody with human ovarian carcinoma. *J Clin Invest* 1981; 86:1331–1337.
6. Kenemans P, Bast RC, Yedema CA, Price MR, Hilgers J. CA 125 and polymorphic epithelial mucin as serum tumor markers. *Cancer Rev* 1988; 11–12:119–144.
7. Brenner DE, Shaff MI, Jones HW, Grosh WW, Greco FA, Burnett LS. Abdominopelvic computed tomography: evaluation in patients undergoing second-look laparotomy for ovarian carcinoma. *Obstet Gynecol* 1985; 65:715–719.
8. Goldhirsch A, Triller JK, Greiner R, Dreher E, Davis BW. Computed tomography prior to second-look operation in advanced ovarian cancer. *Obstet Gynecol* 1983; 62:630–634.
9. Epenetos AA, Mather S, Granowska M, et al. Targeting of iodine-123-labelled tumour-associated monoclonal antibodies to ovarian, breast, and gastrointestinal tumours. *Lancet* 1982; ii:999–1004.
10. Kenemans P, Yedema CA, Hilgers JHM, et al. Clinical applications of monoclonal antibodies against ovarian cancer-associated antigens. *Eur J Obstet Gynecol Reprod Biol* 1988; 29:207–218.
11. Granowska M, Shepherd J, Britton KE, et al. Ovarian cancer: diagnosis using ^{123}I-monoclonal antibody in comparison with surgical findings. *Nucl Med Comm* 1984; 5:485–499.
12. Symonds EM, Perkins AC, Pimm MV, Baldwin RW, Hardy JG, Williams DA. Clinical implications for immunoscintigraphy in patients with ovarian malignancy: a preliminary study using monoclonal antibody 791T/36. *Br J Obstet Gynecol* 1985; 92:270–276.
13. Jackson PC, Pitcher EM, Davies JO, et al. Radionuclide imaging of ovarian tumours with a radiolabelled (^{123}I) monoclonal antibody ($NDOG_2$). *Eur J Nucl Med* 1985; 11:22–28.
14. Critchley M, Brownless S, Patten M, et al. Radionuclide imaging of epithelial ovarian tumours with ^{123}I-labelled monoclonal antibody (H317) specific for placental-type alkaline phosphatase. *Clin Radiol* 1986; 37:107–112.
15. Haisma HJ, Mosely KR, Kaplan W, Tumek S, Knapp RC. Imaging of ovarian carcinoma with monoclonal antibody OC 125. *Br J Cancer* 1987; 56:4.
16. Hunter RE, Boherty S, Griffin TW, et al. Use of indium-111-labeled OC125 monoclonal antibody in the detection of ovarian carcinoma. *Gyn Oncol* 1987; 27:325–337.
17. Verheijen RHM, Massuger LFAG, Kenemans P, Haisma HJ, Epenetos AA. Polymorphic epithelial mucin and CA125-bearing glycoprotein as targets for imaging and therapy with monoclonal antibodies. *Cancer Rev* 1988; 11–12:145–172.
18. Hagan PL, Halpern SE, Chen A, et al. In vivo kinetics of radiolabeled monoclonal anti-CEA antibodies in animal models. *J Nucl Med* 1985; 26:1418–1423.
19. Poels LG, Peters D, Van Megen Y, et al. Monoclonal antibody against human ovarian tumor-associated antigens. *J Natl Cancer Inst* 1986; 76:781–791.
20. Epenetos AA, Lavender J, Kenemans P, Poels LG. Early results of the monoclonal antibody OV-TL 3 in specific detection of ovarian cancer. *J Clin Oncol* 1987; 5:160.
21. Kühnel R, Rao BR, Poels LG, Delemarre JFM, Kenemans P, Stolk JG. Multiple parameter analyses of human ovarian cancer: morphology, immunohistochemistry, steroid hormone receptors and aromatase. *Anticancer Res* 1988; 8:281–286.
22. Boerman OC, van Niekerk CC, Makkink K, Hanselaar AGJM, Kenemans P, Poels LG. A comparative immunohistochemical study of four monoclonal antibodies directed against ovarian carcinoma associated antigens. *Int J Gynecol Pathol* 1990:in press.
23. Taylor-Papadimitriou J, Peterson J, Arklie J, Burchell J, Ceriani RL, Bodmer WF. Monoclonal antibodies to epithelial-specific components of the human milk fat globule membrane: production and reaction with cells in culture. *Int J Cancer* 1981; 28:17–21.
24. Hnatowich DJ, Childs RL, Lanteigne D, Najafi A. The preparation of DTPA-coupled antibodies radiolabeled with metallic radionuclides: an improved method. *J Immunol Meth* 1983; 65:147–157.

25. Hamilton TC, Young RC, Louie KG, et al. Characterization of a xenograft model of human ovarian carcinoma which produces ascites and intraabdominal carcinomatosis in mice. *Cancer Res* 1984; 44:5286–5290.
26. Giacomini P, Natali P, Ferrone S. Analysis of the interaction between a high molecular weight melanoma-associated antigen and the monoclonal antibodies to the distinct antigenic determinants. *J Immunol* 1985; 135:696–708.
27. Henzen-Logmans SC, Schipper NW, Poels LG, Kenemans P, Meyer CJLM. Use of statistical evaluation of antigen profiles in differential diagnosis between colonic and ovarian adenocarcinomas. *J Clin Pathol* 1988; 41:644–649.
28. McKay DR, Bautovich GJ, Wilson MR, Walker KZ. The effect of circulating antigen on radioimmunodetection and monoclonal antibody localisation: studies in a normal rat model. *Eur J Nucl Med* 1989; 15:313–320.
29. Baum RP, Hernaiz Driever P, Drahovsky D, Hor G. A rapid method for the determination of human CEA/mouse anti-CEA immune complexes in patients undergoing immunoscintigraphy. *Eur J Nucl Med* 1989; 15:321–325.
30. Wahl RL, Parker CW, Philpott GW. Improved radioimaging and tumor localization with monoclonal $F(ab')_2$. *J Nucl Med* 1983; 24:316–325.
31. Fairweather DS, Bradwell AR, Dykes PW, Vaughan AT, Watson-James SF, Chandler S. Improved tumour localisation using indium-111-labelled antibodies. *Br Med J* 1983; 287:167–170.
32. Perkins AC, Pimm MC. Differences in tumour and normal tissue concentrations of iodine- and indium-labelled monoclonal antibody. I. The effect on image contrast in clinical studies. *Eur J Nucl Med* 1985; 11:295–299.
33. Gitsch E, Pateisky N, Philipp K. Radical isotope surgery: an enrichment for the surgical therapy of gynecological malignancies. *Eur J Gynaec Oncol* 1987; 8:71–75.
34. Barzen G, Mayr AC, Langer M, et al. Radioimmunoscintigraphy of ovarian cancer with ^{131}I-labeled OC-125 antibody fragments. *Eur J Nucl Med* 1989; 15:42–48.
35. Chatal JF, Fumoleau P, Saccavini JC, et al. Immunoscintigraphy of recurrences of gynecologic carcinomas. *J Nucl Med* 1987; 28:1807–1819.
36. Morrel EM, Tompkins RG, Fischman AJ, et al. Autoradiographic method for quantitation of radiolabeled proteins in tissues using indium-111. *J Nucl Med* 1989; 30:1538–1545.
37. Carrasquillo JA, Abrams PG, Schroff RW et al. Effect of antibody dose on the imaging and biodistribution of indium-111-9.2.27 anti-melanoma monoclonal antibody. *J Nucl Med* 1988; 29:39–47.
38. Haisma HJ, Mosely KR, Bataile A, Griffiths TC, Knapp RC. Distribution and pharmacokinetics of radiolabeled monoclonal antibody OC 125 after intravenous and intraperitoneal administration in gynecologic tumors. *Am J Obstet Gynecol* 1988; 159:843–848.